Supplementary Information

Moisture-based green energy harvesting over 600 hours via photocatalysis-enhanced hydrovoltaic effect

Peng Duan[1], Chenxing Wang[1], Yinpeng Huang[1], Chunqiao Fu[1], Xulei Lu[1], Yong Zhang[1], Yuming Yao[1], Lei Chen[1], Qichang He[1,3], Linmao Qian[1], Tingting Yang✉[1,2]

1 Tribology Research Institute, School of Mechanical Engineering, Southwest Jiaotong University, Chengdu 610031, PR China.
2 Institute of Smart City and Intelligent Transportation, Southwest Jiaotong University, Chengdu 611756, PR China.
3 MSME, Univ Gustave Eiffel, CNRS UMR 8208, F-77454 Marne-la-Vallée, France.

*Corresponding authors. ✉email: yangtingting@swjtu.edu.cn

This PDF file includes:

Supplementary Figures 1-21;

Supplementary Tables 1-3;

Supplementary References.

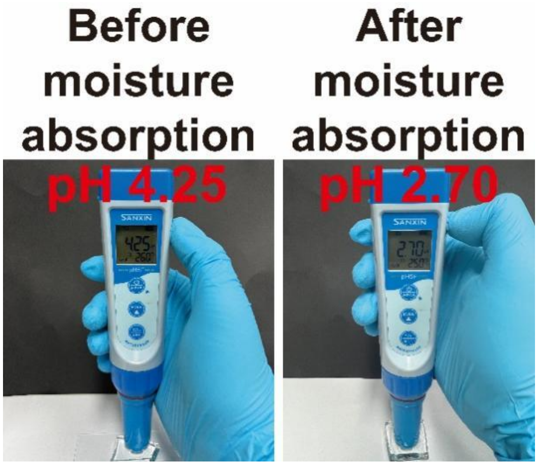

Supplementary Figure 1. Comparison of pH value. Comparison of pH value of gel before and after moisture absorption

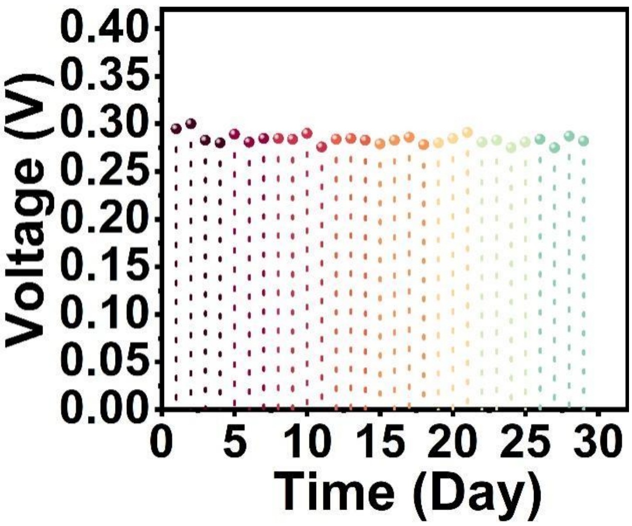

Supplementary Figure 2. Long-term voltage test of MEG. MEG can maintain stable voltage output for a long time in a humid environment (98% RH, 25 ℃).

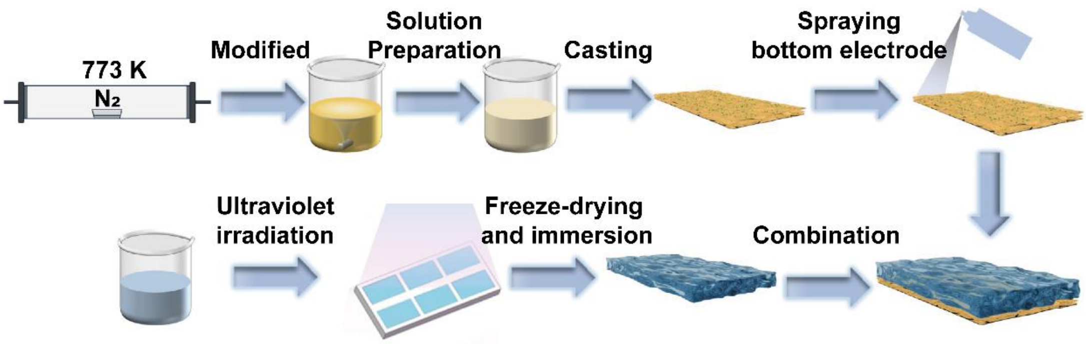

Supplementary Figure 3. Preparation process. Flow chart for the preparation of MEL-PCL structure

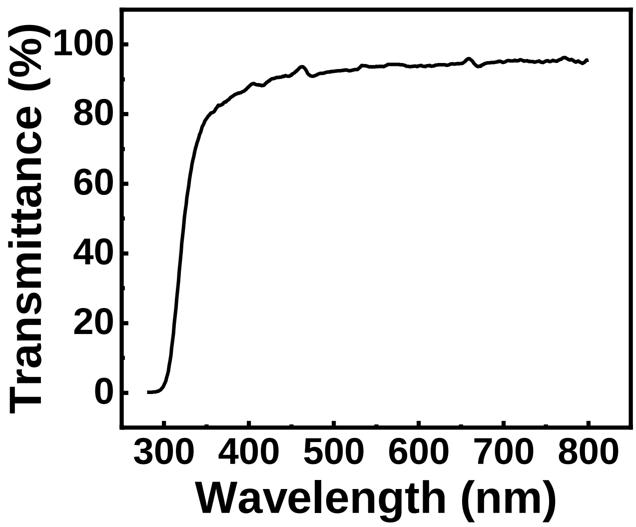

Supplementary Figure 4. Light transmittance rate of the MEL. MEL has good light transmittance in the range of 400-800nm.

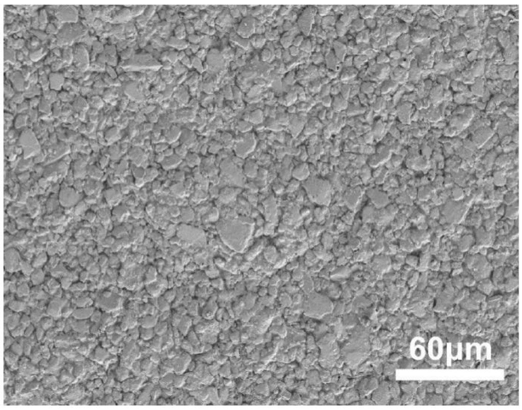

Supplementary Figure 5. Morphology of carbon nitride on the back of the PCL. Carbon nitride is evenly distributed. Such a distribution can provide a large number of photocatalytic sites.

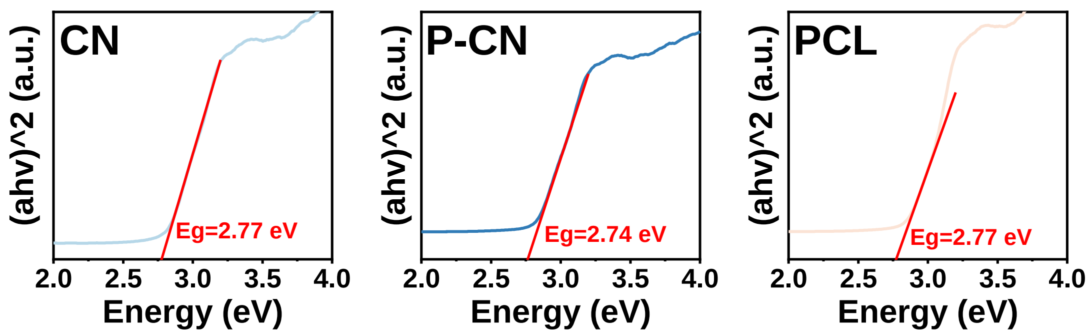

Supplementary Figure 6. Tauc plots of CN, P-CN and PCL. $E_{VB} = \chi - E_e + 0.5E_g$, $E_{VB} = E_g + E_{CB}$, Where χ is the absolute electro-negativity of semiconductor, and the χ value of g-C_3N_4 is 4.73 eV, The free electron energy is denoted as E_e (4.5 eV vs NHE).

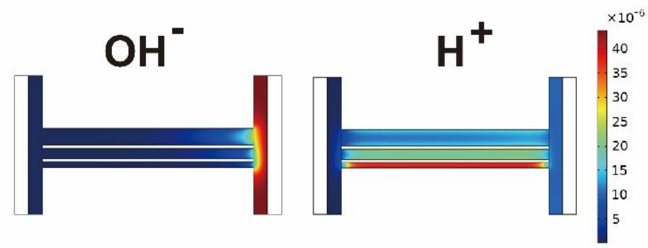

Supplementary Figure 7. Simulation of cation selectivity. The concentration of H^+ and OH^- in the left solution is 10^{-7} mol/L, and the concentration of the right solution is 0.01 mol/L. The nanopore channels are negatively charged, with the sizes of 240 nm, 150 nm, and 80 nm, respectively. The system is stabilized in such a way that the nanopore channels allow only H^+ to pass through them, which is cation-selective.

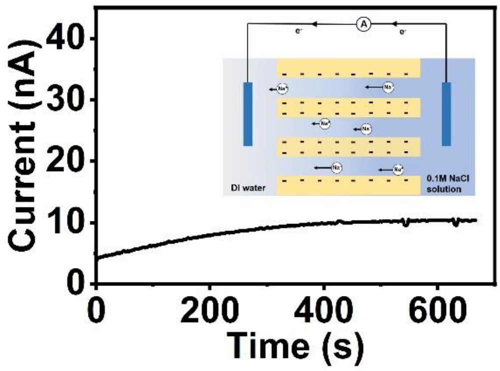

Supplementary Figure 8. Experiment of cation selectivity. The left liquid is deionized water, the right is a 0.1 mol/L NaCl solution, the membrane in the middle is a PCL, and the left side of the system is the positive electrode of the current, the membrane is capable of selectively transmitting cations.

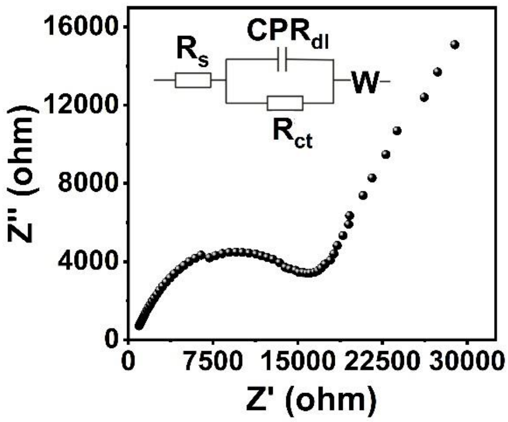

Supplementary Figure 9. Impedance analysis of the device. The illustration is the equivalent circuit diagram of the device.

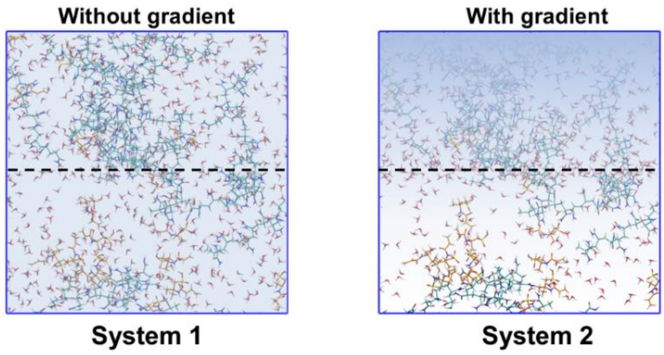

Supplementary Figure 10. Simulation systems. Initial conformation of the simulation system before and after illumination

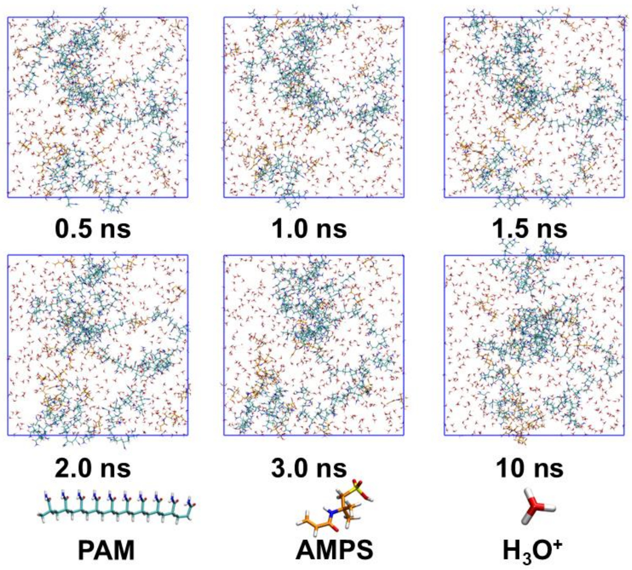

Supplementary Figure 11. H_3O^+ density distribution change of system 1. H_3O^+ do not move in a directional manner in system 1.

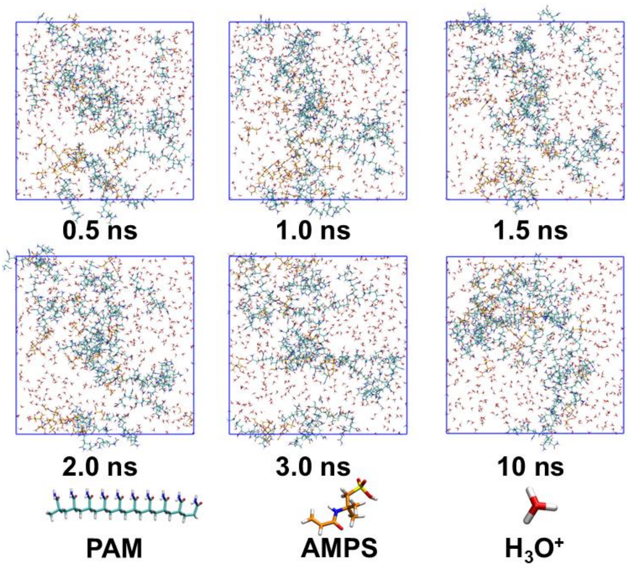

Supplementary Figure 12. H_3O^+ density distribution change of system 2. H_3O^+ moves in a directional manner in system 2.

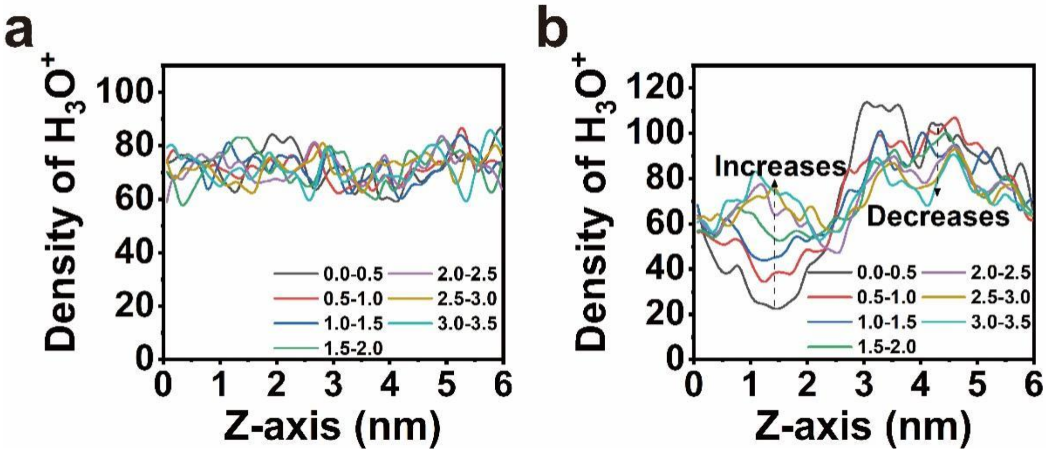

Supplementary Figure 13. Density change of H_3O^+. a Density change of H_3O^+ in the absence of concentration gradient **b** Density change of H_3O^+ when there is a concentration gradient. Different colors mark the average density of the system along the Z axis (concentration gradient direction) in each time period (ns).

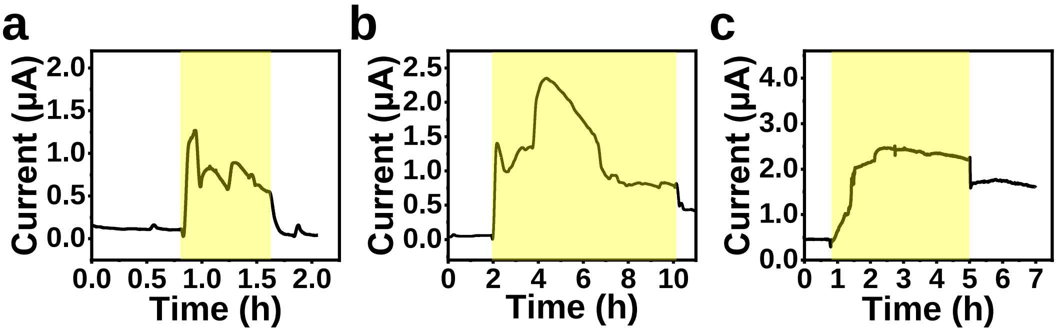

Supplementary Figure 14. Effect of illumination time on device performance recovery. **a** short illumination (1 h), **b** medium illumination (4 h) **c** long illumination (8 h)

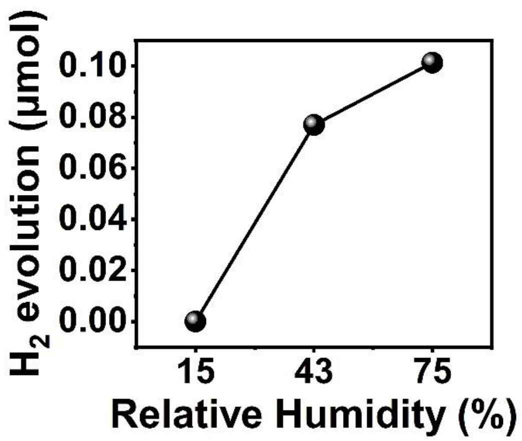

Supplementary Figure 15. Effect of relative humidity on photocatalytic effect. Hydrogen production of the device at different humidity levels for 4 hours

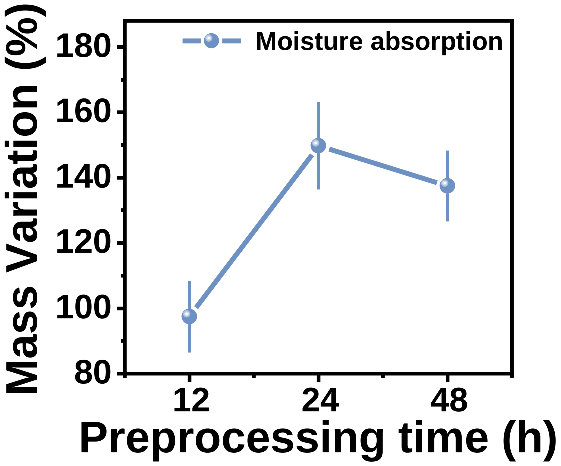

Supplementary Figure 16. Effect of preprocessing time. Effect preprocessing time in LiCl solution on the moisture absorption capacity of the MEL.

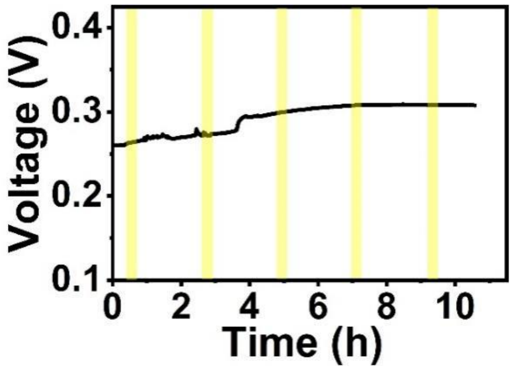

Supplementary Figure 17. Voltage repeatability test under illumination. Voltage responses during five illumination cycles.

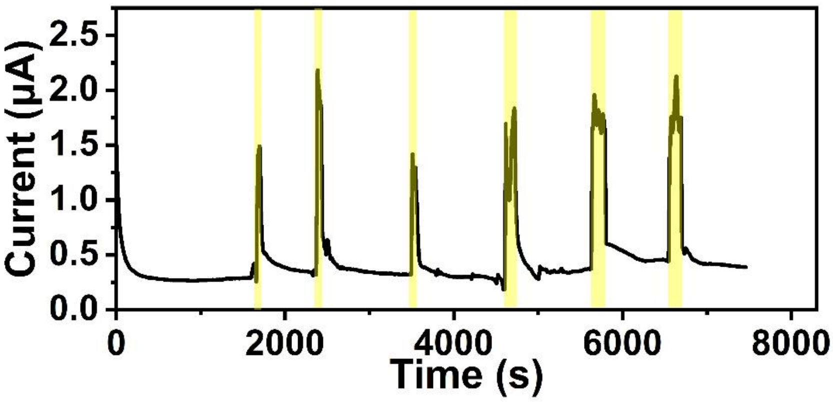

Supplementary Figure 18. Current repeatability test under illumination. Current responses during six illumination cycles.

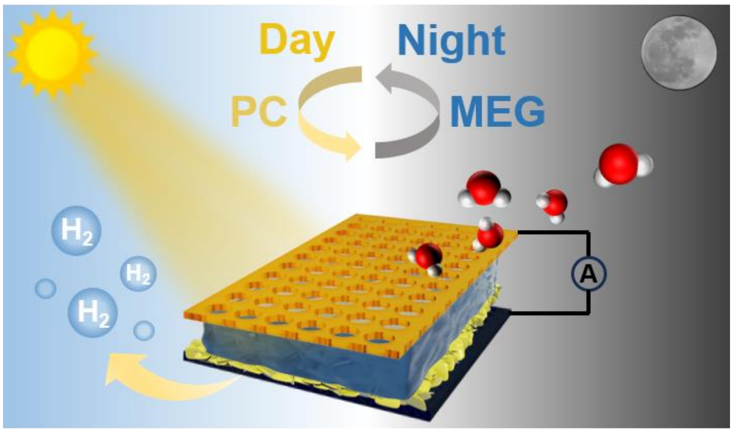

Supplementary Figure 19. Application prospects. Schematic diagram of the device for day-night cycle power generation (The device can generate electricity using hydrogen ion concentration at night, and can reconstruct the internal hydrogen ion concentration gradient under the action of light during the day, thus achieving day and night cycle power generation.).

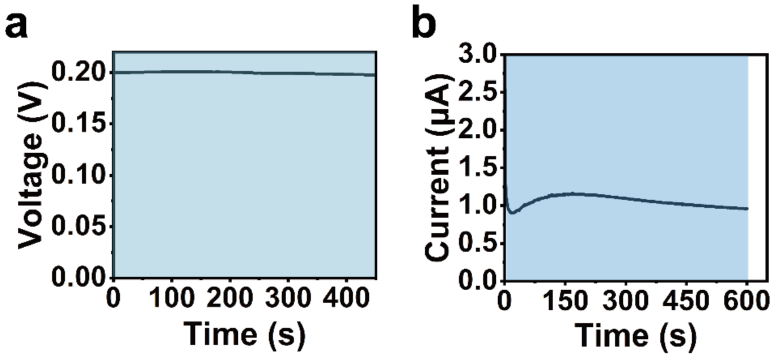

Supplementary Figure 20. Low temperature test. a Voltage output of the device at -20°C (the blue part is a low temperature environment) **b** Current output of the device at -20°C (the blue part is a low temperature environment)

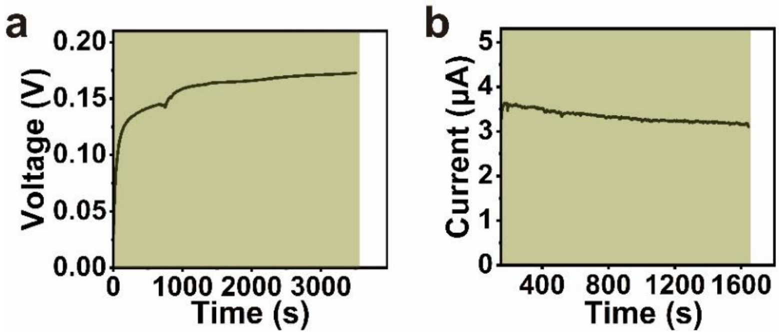

Supplementary Figure 21. Anti-pollution ability test. a Voltage output of the device when it is covered with soil (the brown part is the soil-covered environment) **b** Current output of the device when it is covered with soil (the brown part is the soil-covered environment)

Supplementary Table 1 | Comparison of performance parameters of MEG devices

V_{oc} (V)	I_{sc}/ J_{sc}	Continuous working time	Ref	Electrode
1.0	1.79μA/cm^2	4.17h	1	C
0.78	7.5μA	240h	2	C
0.91	50.07μA	11.1h	3	Au
1.1	17nA	11.7h	4	C
0.4	1.5 μA/cm^2	8.3h	5	Au
0.6	50nA	258h	6	C
0.5	0.25μA	140h	7	Reassembled Graphite
0.28	1.8μA	650h	This work	Au
0.9	92μA/cm^2	24h	8	Cu
0.8	20μA	12h	9	Cu
0.4	0.12μA	8h	10	ITO
1.1	2.6μA/cm^2	13.9h	11	C-Al
1.17	400μA	10h	12	Al
0.4	5.7μA	3.3h	13	Ag
1.04	610μA	/	This work	Al

Supplementary Table 2 | Photocatalytic hydrogen production data of our devices

Time (h)	Peak area (uV*s)	H_2 evolution (μmol)
0	0	0
1	4538.6	2.64722
2	5871.3	3.424541
3	6215.6	3.62536
4	11599.3	6.7655

Supplementary Table 3 | Electrochemical impedance spectroscopy results of MEG

R_s (Ω)	C_d (uF/cm^2)	n	R_{ct} (Ω)	W
408.9	5.036	0.594	14610	$2.233*10^{-5}$

Supplementary References

1 He, W. *et al.* Textile-based moisture power generator with dual asymmetric structure and high flexibility for wearable applications. *Nano Energy* **95**, 107017 (2022).

2 Tan, J. *et al.* Self-sustained electricity generator driven by the compatible integration of ambient moisture adsorption and evaporation. *Nat. Commun.* **13**, 3643 (2022).

3 Li, P. *et al.* Multistage coupling water-enabled electric generator with customizable energy output. *Nat. Commun.* **14**, 5702 (2023).

4 Zhao, K. *et al.* Moisture-driven energy generation by vertically structured polymer aerogel on water-collecting gel. *Nano Energy* **126**, 109645 (2024).

5 Long, Y. *et al.* Moisture-induced autonomous surface potential oscillations for energy harvesting. *Nat. Commun.* **12**, 5287 (2021).

6 Wang, H. *et al.* Bilayer of polyelectrolyte films for spontaneous power generation in air up to an integrated 1,000 V output. *Nat. Nanotechnol.* **16**, 811-819 (2021).

7 Moreira, K. S. *et al.* Flexible, low-cost and scalable, nanostructured conductive paper-based, efficient hygroelectric generator. *Energy Environ. Sci.* **14**, 353-358 (2021).

8 Mo, J. *et al.* Sulfated cellulose nanofibrils-based hydrogel moist-electric generator for energy harvesting. *Chem. Eng. J.* **491**, 152055, doi:10.1016/j.cej.2024.152055 (2024).

9 Huang, Y. *et al.* Three-Dimensional Printing of High-Performance Moisture Power Generators. *Adv. Funct. Mater.* **34**, 2308620 (2024).

10 Yang, Y. n. *et al*. Moisture-Electric–Moisture-Sensitive Heterostructure Triggered Proton Hopping for Quality-Enhancing Moist-Electric Generator. *Nano-Micro Lett.* **16**, 56 (2024).
11 He, T. *et al.* Fully printed planar moisture-enabled electric generator arrays for scalable function integration. *Joule* **7**, 935-951 (2023).
12 Cao, Y.-M. *et al.* Vertical Phase-Engineering MoS2 Nanosheet-Enhanced Textiles for Efficient Moisture-Based Energy Generation. *ACS Nano* **18**, 492-505 (2023).
13 He, W. *et al.* Robustly and Intrinsically Stretchable Ionic Gel-Based Moisture-Enabled Power Generator with High Human Body Conformality. *ACS Nano* **18**, 12096-12104, doi:10.1021/acsnano.3c08543 (2024).